

# Composite Flywheel Design for a Magnetically Suspended Flywheel Energy Storage System

D. PANG,<sup>1</sup> D. M. RIES,<sup>2</sup> C. M. LASHLEY,<sup>2</sup> J. A. KIRK<sup>1</sup> AND D. K. ANAND<sup>1</sup>

## ABSTRACT

This paper presents a study of designing, manufacturing and testing of the composite flywheel for magnetically suspended flywheel energy storage system. The study includes the rotor material selection, rotor performance analysis, rotor design and specifications, rotor fabrication and composite material test methods. Carbon fiber and epoxy resin are used for the composite flywheel to achieve high specific energy density (SED). The flywheel includes one metal ring and five composite rings. The composite rings are interference assembled to provide an optimum stress distribution at high speed. An optimal design and specifications of the flywheel are suggested. Wet filament winding and oven curing are used to fabricate the flywheel. Test methods for mechanical properties and composite quality are investigated.

## INTRODUCTION

The University of Maryland has developed a magnetically suspended flywheel energy storage system integrating the magnetic bearing, motor/generator and composite flywheel. The system offers high efficiency, large stored energy, low weight and minimal maintenance. It can provide a high usable specific energy density (SED) of 20 WH/Kg and long lifetime of 10 to 15 years, which is very attractive for spacecraft applications. The proposed system was designed for a low earth orbit satellite with a 90 minute cycle. The flywheel is accelerated and stores energy during the 60 minute interval when the satellite is exposed to the sunlight. The flywheel is spun down and releases energy during 30 minute interval when the satellite is in the darkness.

A prototype using two magnetic bearings, a permanent magnet brushless motor/generator and an aluminum flywheel was designed, built and tested [1]. The permanent magnet/electromagnet (PM/EM) magnetic bearings were used for axially supporting the flywheel and radially controlling its position. The motor/generator was mounted between two magnetic bearings to store and retrieve energy from the flywheel. Figure 1 shows a stack arrangement of the flywheel energy storage system. The aluminum flywheel was used in the prototype for testing purpose. It will be replaced by a composite flywheel in the future [2].

---

<sup>1</sup> Department of Mechanical Engineering, University of Maryland, College Park, MD 20742, USA

<sup>2</sup> Fare, Inc., University Center, 4716 Pontiac St., Suit 304, College Park, MD 20740, USA

## FLYWHEEL CONSIDERATION

Kirk et al [3] has investigated a variety of flywheel configurations and has concluded that a pierced disk, with no spokes and no center shaft, represents a very desirable geometry for flywheel energy storage applications. The specific energy density (SED), the stored energy per unit weight, is a figure of merit in flywheel design. A high SED value implies that a flywheel can store a large amount of energy with a relatively small amount of rotating weight. The SED also can be written in term of the material strength  $\sigma$  and weight density  $\gamma$

$$SED = K_s (\sigma/\gamma)$$

where  $K_s$  is a shape factor that varied between 0 and 1.

Composite materials having a high tensile strength and low weight density are good candidates for flywheel applications. Carbon/epoxy composite material shows its SED almost ten times better than high strength carbon steels.

To further improve performance, the flywheel uses an interference assembled multi-ring design. Figure 2 shows the nondimensional stress distribution of the two ring assembly. The stress distribution due to rotation is indicated by the solid line. In the flywheel design the composite filaments are oriented in the tangential direction so the radial stress reaches the material limit well before the tangential stress reaches its limit. The stress distribution due to the combination of interference and rotation is shown in dashed line. The interference assembly reduces the radial stress and levels the tangential stress. This allows a given flywheel to rotate at a higher speed before either the radial or tangential stress reaches its limit.

The proposed flywheel design includes one metal ring and five composite rings. The composite rotor is filament wound and interference assembled to improve performance. The inner metal ring, which attached to the inside of the rotor, consists of the magnetic bearing return rings, the motor/generator magnet assembly, the touchdown surface, the spacers and the sensor target.

The following design topics are addressed in this paper

- Composite material selection
- Rotor performance analysis
- Rotor design and specifications
- Rotor fabrication
- Composite material test methods

## COMPOSITE MATERIAL SELECTION

Carbon fiber and high performance epoxy matrix are chosen for the rotor because of high strength, high modulus and low weight. Composite materials are extremely resistant to fatigue failure, stress corrosion and stress rupture failure. Experimental studies of unidirectional graphite/epoxy composite have shown the fatigue endurance limit is approximately 70% of the static strength at  $10^5$  cycles. In the flywheel design, which will be discussed below, the stress at the maximum operating speed is only 56% of the maximum stress. The expected lifetime of the flywheel is at least  $10^5$  cycles, about 17 years with a 90 minute cycle time.

After comparing various commercial available carbon fibers Amoco Thornel T-40 was chosen for its high axial tensile strength of 5.65 GPa (820 Ksi). The Amoco fiber is a continuous length, high modulus fiber consisting 12,000 filaments in one ply. The fiber has been sized to increase the composite interlaminar shear strength in an epoxy resin. Shell EPON 828 epoxy resin and Shell z type hardener were selected with the Amoco T-40 fiber to form the composite material. The resin has a tensile strength of 70 MPa (10 Ksi) with a modulus of elasticity greater than 2.75 GPa (400 Ksi). The composite material axial tensile strength can be estimated using the rule of mixtures. The composite has a 62% fiber volume fraction, therefore the axial tensile strength of the composite material is 3.5 GPa (508 Ksi).

## ROTOR PERFORMANCE ANALYSIS

FLYANS and FLYSIZE computer software [4] developed by the University of Maryland was used to design and analyze the composite flywheel. The design variables for the rotor include: the inner diameter, outer diameter, height, assembly interference, number of rings, operating speed, assembly force, gap growth, stored energy, stresses and rotor weight. The design parameters are the rotor material properties. The objective is to maximize the SED. The system constraints are listed as the following

- (1) The minimum inner diameter and height of the rotor are defined by the size of the motor/generator and magnetic bearings.
- (2) The operating speed ratio of the motor/generator is designed to be 2:1.
- (3) The gap growth of the rotor due to the stress should be minimum to avoid any effect on the control system.
- (4) The flywheel weight should be minimum.
- (5) The maximum stress should be less than the fatigue endurance limit and the strength of the rotor material.
- (6) The SED and the stored energy should meet minimum requirements.
- (7) The assembly force should be achieved by the conventional presses without damaging the rings.

Lashley et al [5] found an optimal design of the flywheel with a inner diameter/outer diameter ratio of 0.45, an assembly interference of 0.6% and an operating speed range between 37.5% and 75% of the maximum speed.

## ROTOR DESIGN AND SPECIFICATIONS

The final design of the composite flywheel consists of one inner metal ring and five composite rings with a total weight of 15.2 Kg (33.5 lb). The flywheel can store a usable energy of 975 WH with a useable SED of 65 WH/Kg, when operating between 40,000 and 80,000 RPM. The gap growth will vary between 0.107 mm and 0.429 mm (0.004 and 0.017 inch). The inner metal ring and the first composite ring has no interference. The rest of the rings will be tapered to allow adjacent rings to be interference assembled. The details of the flywheel design are listed in Table 1.

## ROTOR FABRICATION

Three main processes involved in the rotor fabrication are filament winding, curing and machining and assembly. Each composite ring is filament wound using carbon fibers and epoxy resin on a mandrel. The rings are cured in an oven to achieve desired properties. Finally the composite rings are machined to the design dimensions for assembly.

Wet filament winding process is used. The continuous carbon fibers are fed from a large unspliced spool through a resin bath to be impregnated with the epoxy resin. With the mandrel rotating at a constant speed, the carriage holding the payout eye moves back and forth to guide the fibers on to the mandrel as shown in Figure 3. To optimize the flywheel performance the hoop winding pattern keeps the helix angle of the winding near 90 degrees. Fiber tension must be controlled to minimize the residual stress. A magnetic particle brake tensioner is utilized to maintain a constant tension.

Compared to prepreg winding, wet filament winding has a large number of possible combinations of reinforcements and matrix materials to meet design requirements. Wet filament winding uses oven cure and prepreg winding must use an autoclave. Composite rings must be rotated during curing process to avoid sagging. It is easier and less expensive to implement rotation in an oven than an autoclave. Also, the wet filament wound parts will contain less trapped air to form voids. One difficulty in wet winding is control of precise resin content, which is a function of the resin viscosity, fiber tension, the number of layers per unit thickness, and mandrel diameter. The optimum resin content can only be obtained by testing experimentally.

During the curing process the composite rings are heated up to 175 °C (350 °F) and then cool down. The key parameters for the process are time, temperature, heat-up/cooling-down rate and vacuum pressure. Vacuum bagging technology is utilized to remove any trapped air and consolidate the composite mass. A thermocouple is used in the cure oven to control the temperature profile of the curing process. During the curing process the composite winding is rotated to prevent any sags and keep an even fiber/resin distribution. Figure 4 shows a typical cure cycle using vacuum bagging techniques.

The composite rings will be machined to the design dimensions using conventional machines such as lathes and milling machines. The use of diamond or carbide tipped tool is recommended and the cutting tools should be kept sharp to minimize delamination. Cooling or lubrication is necessary to prevent resin built up on the cutting tool to overheat the parts. The optimal cutting speed and feed rate can vary depending on the fiber/resin ratio and the thickness of the composites. Typical values for machining are a cutting speed of 180 to 300 mm/min (600 to 1000 ft/min) and a feed rate of 0.05 to 0.13 mm/rev (0.002 to 0.005 in/rev). Based on the past laboratory studies the dimensional tolerance of the composites can be achieved within 0.025 mm (0.001 inch). Once the composite rings are machined to the desired shapes they will be pressed together using Shell epoxy as a lubricant.

## COMPOSITE MATERIAL TEST METHODS

Traditionally material properties can be obtained from handbook or manufacturer's data. This approach is not practical for composite materials because of large scatter. Although some properties can be estimated by analytical methods, experiments are still required to validate the data and ensure the quality of the composite material.

Furthermore, the flywheel shape is considerably different from a flat specimen used in the standard tests. The important material properties include: tangential and radial moduli, Poisson's ratio, tangential tensile and compressive strengths, radial tensile and compressive strengths, shear strength and weight density. The properties for material quality are the fiber volume fraction, void content and fiber residual stress. A survey of the test methods [2] found some applicable ASTM standards. The rest of the properties can be obtained by some modification of the standard tests.

The standard test method for tensile strength of the ring is the split disk method, which is described in ASTM standard D-2290 and D-2291. This method measures the maximum load applied on the ring to determine the tangential tensile strength. In order to find the tangential elastic modulus, a strain gage is mounted on the ring to measure the strain as the load is applied. The elastic modulus can be determined by calculating the slope of the linear portion of the stress-strain curve. The composite shear strength is determined using ASTM standard D-2344. The radial tensile strength, transverse to the fiber direction, can be found using the ASTM standard D-2105. The strength can be determined by pulling a long circumferential wound tubular specimen in the longitudinal direction. The radial elastic modulus can be determined with a strain gage on the specimen. ASTM standard D-2586 can be used to find the standard radial compressive strength. Poisson's ratio is best measured on a flat specimen. The test specimen can be cut from the filament wound ring before curing and then cured flat.

Fiber volume fraction is the percentage of fibers in a unit volume. Variations in volume fraction affect final mechanical and physical properties. The fiber volume fraction is a function of resin viscosity, fiber tension, winding speed, mandrel diameter and stiffness, the number of layers per unit thickness, curing temperature and vacuum pressure. A test program is needed to determine the effects of these variables on fiber volume fraction. ASTM standard D-3171 is an accurate method to measure the fiber volume fraction.

Voids in a composite significantly affect its mechanical properties. A composite with voids will have greater scatter in its strength measurement. The voids will lower the fatigue strength and make the composite more susceptible to moisture inclusion. From a quality control viewpoint the void content is very important. ASTM standard D-2734 describes a method for determining the void content. A well made composite contains less than 1% voids [6].

Residual stresses are induced in a composite part as a result of the fabrication and curing processes. The residual stress can be determined by cutting a ring through its cross section. The ring will open or close depending upon the residual stress state inside the ring. A closing ring implies a tensile residual stress near the inner diameter and a compressive stress near the outer diameter. Figure 5 shows the calculations and method used to determine the residual stresses in a wound composite ring [7].

## CONCLUSIONS

A study of the designing, manufacturing and testing of the composite flywheel was conducted. Carbon fiber and epoxy resin are chosen for the composite material of the rotor because of their high strength and low weight. An optimal design of the flywheel for the energy storage is suggested. Wet filament winding with an oven

curing are used to manufacture the composite rings. The rings will be machined to the desired dimensions and interference assembled together. Several test methods for mechanical properties and composite quality for tubular ring-shaped composites are surveyed. Few composite rings have been made and are ready for testing. To ensure the quality of the composite a further study of factors affecting rotor fabrication is recommended.

## REFERENCE

1. Anand, D. K., Kirk, J. A., Zmood, R. B., Pang, D., Lashley, C., 1991. "Final Prototype of Magnetically Suspended Flywheel Energy Storage System", Proceedings of 26th IECEC, Boston, MA.
2. Ries, C. M., 1991. Manufacturing Analysis for a Composite Multi-ring Flywheel, M.S. Thesis, University of Maryland, College Park, MD.
3. Kirk, J. A., Huntington, R. A., 1977. "Energy Storage - An Interference Assembled Multiring Superflywheel", Proceedings of 12th IECEC, Washington, D.C., 1977.
4. Khan, A. A., 1984. Maximization of Flywheel Performance, M.S. Thesis, University of Maryland, College Park, MD.
5. Lashley, C. M., Ries, D. M., Zmood, R. B., Kirk, J. A., Anand, D. K., 1989. "Dynamics Considerations for a Magnetically Suspended Flywheel", Proceedings of 24th IECEC, Washington, D.C.
6. ASM International, 1987. Engineering Material Handbook, Volume I, Composites, Metals Park, Ohio.
7. Hannibal, A. J., 1982. "Fabrication of High Performance Filament Wound Fiber Composite Rings", Project X882-A-Flywheel Development, Lord Corporation, Erie, PA.

Table 1 Rotor Design and Specifications

Flywheel Design	
Flywheel Length	215.9 mm (8.5 in)
Flywheel Mass	15.2 Kg (33.5 lb)
Maximum Speed	106,000 RPM
Operating Speed Range	40,000 - 80,000 RPM
SED at Maximum Speed	152 Wh/Kg (69 Wh/lb)
Useable SED	65 Wh/Kg (29.2 Wh/lb)
Useable Stored Energy	975 Wh
Gap Growth at Lower Speed	0.107 mm (0.0042 in)
Gap Growth at Upper Speed	0.429 mm (0.0169 in)

Table 1 Rotor Design and Specifications (Cont.)

Flywheel Dimensions				
Ring No.	I.R. Ratio	Inner Radius	Outer Radius	Ring Mass
1	0.426	54.10 mm (2.130 in)	57.15 mm (2.250 in)	1.82 Kg (4.0 lb)
2	0.450	57.15 mm (2.250 in)	71.55 mm (2.817 in)	1.86 Kg (4.1 lb)
3	0.560	71.12 mm (2.800 in)	85.42 mm (3.363 in)	2.27 Kg (5.0 lb)
4	0.670	85.09 mm (3.350 in)	99.39 mm (3.913 in)	2.68 Kg (5.9 lb)
5	0.780	99.06 mm (3.900 in)	113.36 mm (4.463 in)	3.09 Kg (6.8 lb)
6	0.890	113.03 mm (4.450 in)	127.00 mm (5.000 in)	3.50 Kg (7.7 lb)

Flywheel Ring Assembly Specifications			
Ring Assembly	% Interference	Minimum Taper	Assembly Force
3	0.6	0.113 degree	512 N (115 kips)
4	0.6	0.135 degree	641 N (144 kips)
5	0.6	0.157 degree	703 N (158 kips)
6	0.6	0.179 degree	752 N (169 kips)

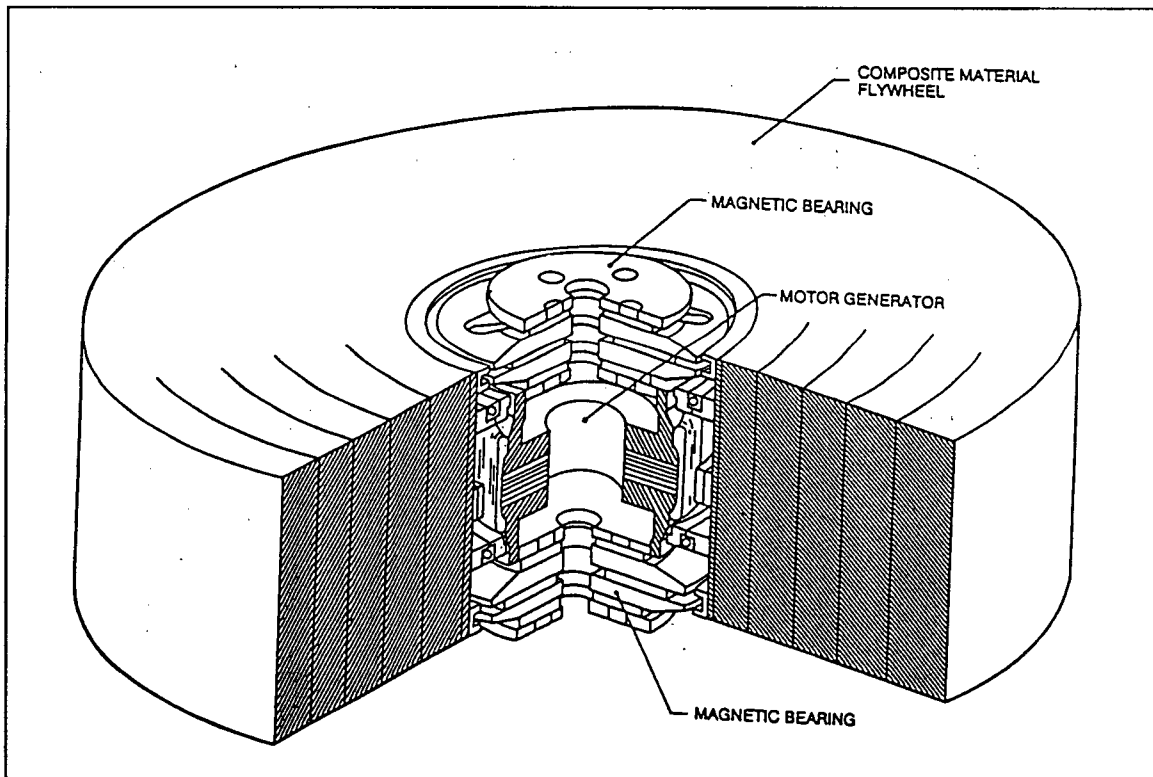


Figure 1 Cut Away Sectional View of Flywheel Energy Storage System

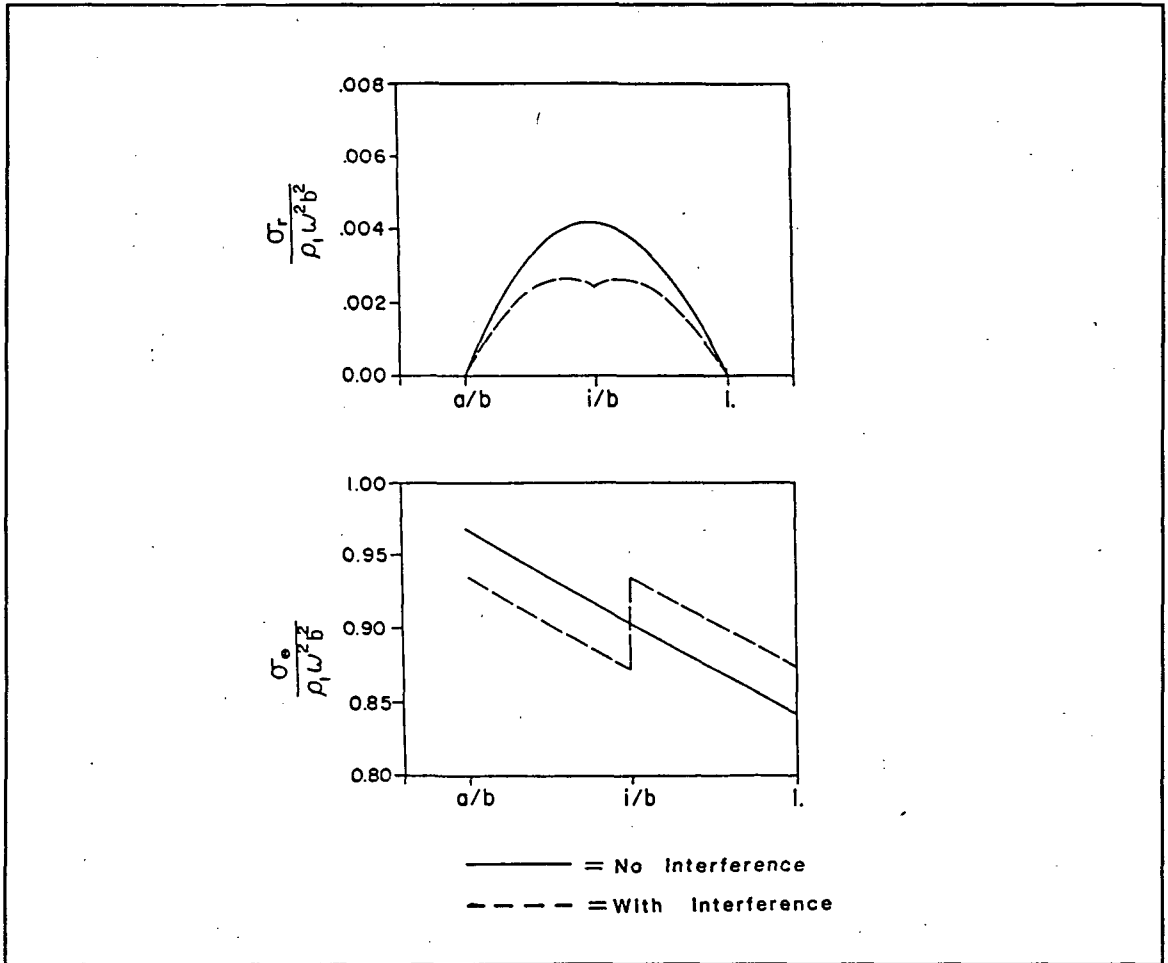


Figure 2 Rotational and Combined Stresses of 2 Ring Assembly

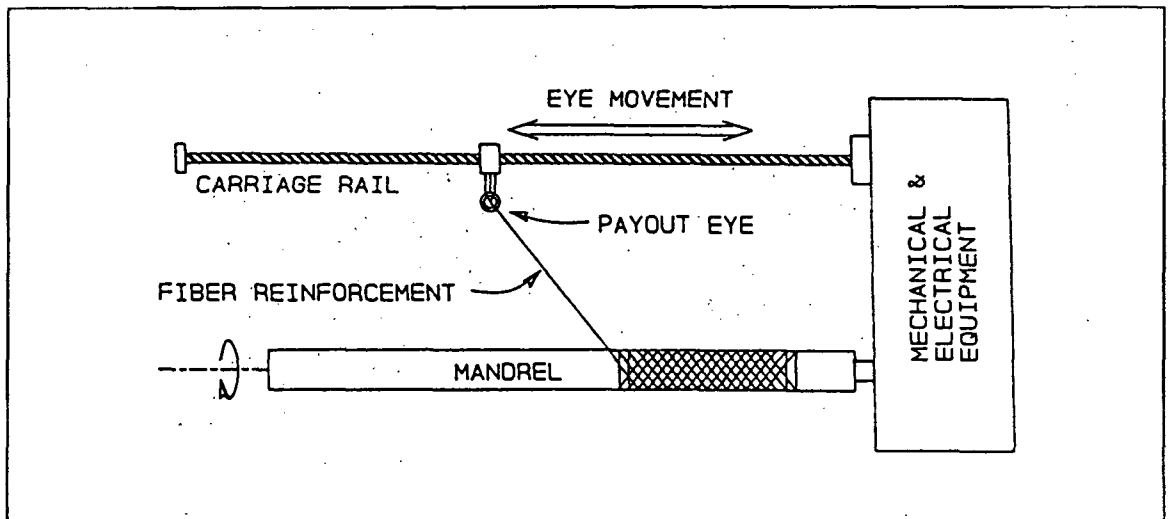


Figure 3 Two Axis Filament Winding Process for Rotor Fabrication

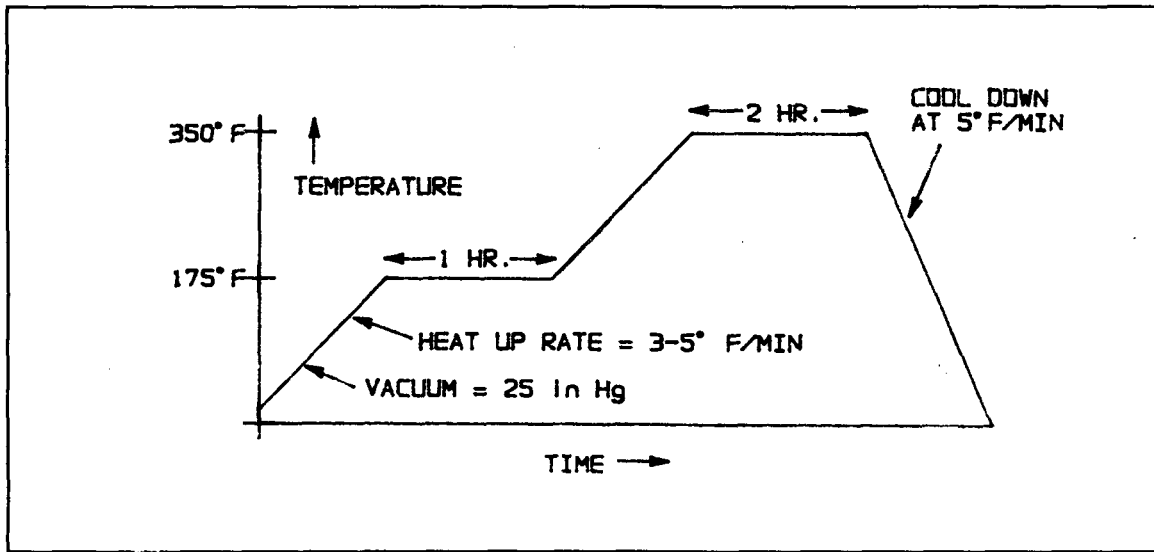


Figure 4 A Typical Epoxy Cure Cycle Using Vacuum Bagging Technique

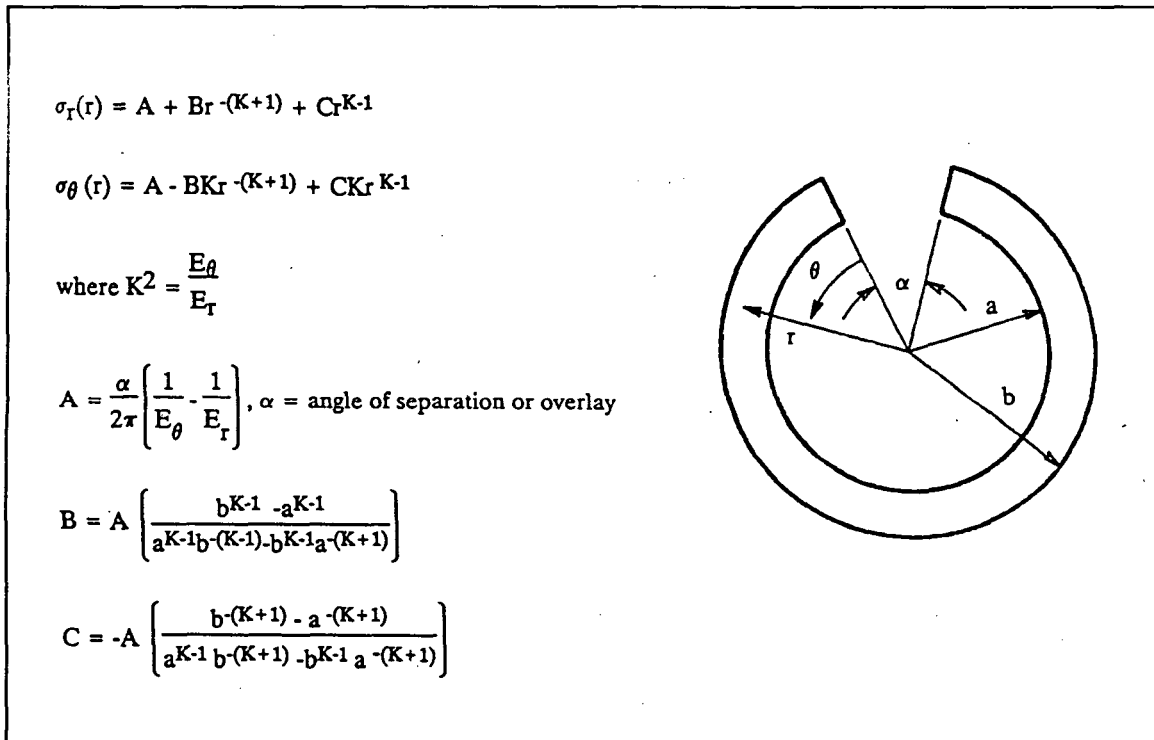


Figure 5 Residual Stresses in a Wound Composite Ring [7]